Structural responses of non-targeted bacterial and hppd communities to the herbicide tembotrione in soil

Hugo Terol, Clémence Thiour-Mauprivez, Marion Devers, Fabrice Martin-Laurent, Marcelino Suzuki, Christophe Calvayrac, Lise Barthelmebs

Structural responses of non-targeted bacterial and *hppd* communities to the herbicide tembotrione in soil.

Hugo Terol[1,2], Clémence Thiour-Mauprivez[3], Marion Devers[3], Fabrice Martin-Laurent[3], Marcelino Suzuki[2], Christophe Calvayrac[1,2], Lise Barthelmebs[1,2*]

[1] *Université de Perpignan Via Domitia, Biocapteurs-Analyse-Environnement, 66860, Perpignan, France*

[2] *Sorbonne Université, CNRS, Laboratoire de Biodiversité et Biotechnologies Microbiennes, LBBM, F-66650, Banyuls-sur-Mer, France*

[3] *Agroécologie, INRAE, Institut Agro, Univ. Bourgogne, Univ. Bourgogne Franche-Comté, F-21000 Dijon, France*

*Corresponding author: barthelm@univ-perp.fr

Abstract:

Tembotrione (TBT) is a β-triketone herbicide targeting the 4-Hydroxyphenylpyruvate dioxygenase enzyme (4-HPPD) of weeds. This molecule can also affect soil microorganisms, either through both direct and indirect toxic effects for microorganisms expressing 4-HPPD, or by promoting tolerant and/or degrading microbial populations. Our study aimed to characterize the impacts of TBT on the diversity of total- and *hppd* (coding for 4-HPPD) -soil bacterial communities. Soil microcosms were treated with the active ingredient TBT at the recommended field dose (100g a.i/ha; D1) or the tenfold dose (D10). Soil samples were collected from 0 to 55 days post-treatment to study: (i) total- and *hppd*-bacterial diversities using 16SrRNA and *hppd* amplicons sequencing, respectively; (ii) TBT dissipation in soil. Both

total- and *hppd*-bacterial community composition was not affected by TBT treatments (D1 and D10). However, D10 treatment slightly increased richness and phylogenetic diversity of the total bacterial community while decreasing *hppd* richness. Overall, the highest dose of TBT seemed to promote TBT-tolerant or TBT-degrading bacterial populations and to deplete TBT-sensitive ones. These effects were transient as TBT was rapidly dissipated with a DT_{50} of 7 days and 15 days for D1 and D10, respectively. Differential abundance analysis with a Generalized Linear Model allowed the identification of *Sphingomonas, Steroidobacter* and *Lysobacter* as genus that were influenced by TBT, and which could be used as a new class of exposure biomarkers.

Keywords: β-triketone, Microbial ecotoxicology, biomarker, HPPD function

1. Introduction

Soil is one of the world's greatest reservoir of microbial diversity and contains the most diverse and abundant groups of organisms on earth (Hicks et al., 2022). Those soil microorganisms are known to live in hot spots, in close contact with all the organic matter naturally present in, or added to the soil, such as plant protection products (PPPs) which are applied in conventional agriculture to increase crop yields and feed an ever-growing population. The Yin and Yang concept has been proposed in the literature to illustrate the potential effects of PPPs exposure on microbial communities (Karpouzas et al., 2016). On the Yang side of the interaction, PPPs could be used as an energy source by a part of the soil microbial community. Whereas on the Yin side, PPPs could exert toxicity on soil microorganisms. Since the effects of PPPs on microbial communities are also highly dependent on both the physicochemical properties of soils and the active ingredient, as these parameters influence PPPs fate and bioavailability (Griffiths & Philippot, 2013), it seems important to consider the ecosystem where

51 microorganism and PPP interactions take place, as proposed by the microbial ecotoxicology
52 approach (Cébron et al., 2022). Among the studies assessing PPPs effects in microbial
53 communities, approximately 30% and 25% of those published from 2000 to today deal with
54 the glyphosate or atrazine respectively (Pubmed research with the following query: (microbial
55 community) AND (herbicide effects)). Moreover, a meta-analysis carried out at three French
56 ministries' request (Ecological Transition, Agriculture, and Research) and led by INRAE and
57 IFREMER between 2020 and 2022, summarized the knowledge on PPPs impacts on
58 biodiversity and ecosystems (Mamy et al., 2022). The authors highlighted the fact that the
59 main herbicide active ingredients applied in agrosystems were poorly studied, except for
60 glyphosate, considered in more than 100 out of the 579 publications studied in the meta-
61 analysis. This statement was particularly true in the case of recently authorized molecules and
62 was the motivation to the current study.

63 Tembotrione (TBT) is a synthetic organic molecule available as a PPP since 2007 and
64 belonging to the β-triketone herbicide family (Group 27 HRAC classification, 2022). This family
65 also includes sulcotrione and mesotrione, released on the market in 1993 and 2001,
66 respectively. In 2020, 970 tons of β-triketone herbicides were sold in the European Union,
67 representing 0.8 % of the total herbicide sales in this region (ec.europa.eu/eurostat). However,
68 despite this low volume and because of their low recommended field dose of application (RfD)
69 (*i.e.*, 100-200 g a.i. / ha), the area of land on which β-triketones are applied is important,
70 representing 4.85 – 9,7 million of ha cropped with corn (ACTA- Les Instituts Techniques
71 Agricoles, France, 2023).
72
73 The toxicity of β-triketones, including TBT, has been evaluated on different isolated model
74 microorganisms by measuring toxicity endpoints (EC_{50} or MIC), with toxicity values ranging
75 from 10 to 100 mg/L (Dumas et al., 2017; Tawk et al., 2015). As for ecotoxicological effects in
76 soil environment, little or no effects have been observed for sulcotrione or mesotrione applied

at the RfD on the abundance, the diversity or the enzymatic activity of soil microbial communities (bacteria, fungi, archaea and photoautotrophs) while applications beyond 5 times the RfD did have impacts, ranging from stimulation of heterotrophic activities to a decrease of cyanobacterial diversity and abundance (Borowik et al., 2017; Crouzet et al., 2010, 2013, 2016; Du et al., 2018; Joly et al., 2012, 2013, 2014; Kaczynski et al., 2016; Pose-Juan et al., 2015; Thiour Mauprivez et al., 2021). Nonetheless, to our knowledge, ecotoxicological effects of TBT on soil microbial communities has not been studied yet.

Recently, new approaches have been proposed to better characterize the effects of pollutants on microbial communities, focusing on the functions they support. Interestingly, in the case of β-triketones, soil bacteria are known to harbor the *hppd* gene, which encodes for 4-Hydroxyphenylpyruvate dioxygenase (HPPD, EC 1.11.13.27) an enzyme targeted by β-triketones (Thiour-Mauprivez et al., 2022). In plants, the HPPD enzyme is involved in plastoquinone and α-tocopherol biosynthesis, two essential photosynthesis cofactors (Moran, 2005). In bacteria, HPPD allows the production of homogentisate from tyrosine, latter transformed in acetoacetate and fumarate in the associated metabolic pathway. Homogentisate could also lead to the production of a brown pigment called pyomelanin through polymerization and oxidation (Pavan et al., 2020). Noteworthy, little is known about the role of HPPD in soil bacteria. Recently, HPPD activity of three environmental bacterial strains have been evaluated with agronomic doses of β-triketone herbicides (including TBT), establishing the existence of sensitive or tolerant populations to the tested molecules (Singh et al., 2018; Thiour-Mauprivez et al., 2022). These interesting results support the suggestions made by some authors to look for tolerant and/or sensitive populations of “non-target microorganisms" that nonetheless carry the enzyme specifically targeted by PPP active ingredient in the frame of environmental risk assessment (ERA); (Petric et al., 2016; Thiour-Mauprivez et al., 2019).

In the current study we evaluated the ecotoxicological impacts of TBT - the most recently authorized β-triketone - on soil bacterial communities. We set up an experimental design where soil microcosms were treated with TBT either at RfD or at 10 times that dose. Treatment with RfD was chosen to assess the impact of TBT on soil microbial communities in a realistic exposure scenario, close to what would happen in treated fields. A tenfold RfD was chosen to assess this impact in a worst-case exposure scenario and to observe effects which couldn't be significant enough at RfD, as it is a common design applied in many ecotoxicological studies of PPPs (Puglisi, 2017). A molecular approach and a high throughput DNA sequencing allowed us to study the structure and the diversity of both the total- and the *hppd*-bacterial community in TBT-treated and control soil microcosms. In addition, to reach European Food Safety Authority (EFSA) goals, willing to integrate new microbial tools for the *a priori* and a *posteriori* ERA, our objective was also to identify microbial groups and bacterial HPPD-containing organisms significantly impacted by TBT applications, which could be used as new biomarkers sensitive to TBT. The exposure scenario was also evaluated by following the dissipation of the active ingredient in soil microcosms over time.

2. Materials and Methods

2.1. Chemicals

TBT (≥ 98 % purity, PESTANAL®, weak acid, pKa = 3.2 and MW = 440.8 g/mol) was purchased from Sigma-Aldrich, France. Dichloromethane (DCM), methanol (MeOH), acetonitrile (ACN), and water for pesticide analyses were pesticide analysis grade and purchased from VWR (France). Acetic acid (glacial, HPLC quality) was purchased from Carlo Erba. For all the other analyses, distilled water was used.

2.2. Soil microcosms and experimental design

2.2.1. Soil sampling

Soil samples were collected from the surface layer (0-20 cm) of an experimental arable field with no previous herbicide treatment, located at the University of Perpignan Via Domitia, France (coordinates: 42°40'55.2"N, 2°53'49.2"E). Soil was sieved to 2 mm, remaining vegetal matter was discarded and soil moisture was measured by weighting soil samples before and after drying at 100°C (6.5 % of dry weight, % dw). Soil samples were stored for one week at 4°C in the dark, prior to use. Thiour-Mauprivez and collaborators used soil from the same field in a previous study and characterized soil composition. It is composed of 16.2% clay, 29.1% silt, and 54.7% sand (sandy loam soil). It contains 27.5 g/kg of organic matter, 15.99 g/kg of organic carbon and 1.25 g/kg nitrogen. Cation Exchange Capacity (CEC) is of 99 meq/kg, Ca^{2+}/CEC of 260.3% and pH of 8.04 (Thiour-Mauprivez et al., 2021).

2.2.2. Microcosm set up

Soil microcosms were made of 20 g of the sampled soil with relative humidity maintained at 20 % (% dw) in rectangular, lidded, plastic boxes. The soil underwent a 1-week period of pre-incubation at 21 ± 2 °C in the dark before the microcosm setup. Subsets of 2 g of soil were placed in 50 mL conical polypropylene tubes and were treated with 300 µL of concentrated TBT solubilized in MeOH or with 300 µL of MeOH only for controls (D0, control). The concentration of TBT solutions was chosen to treat soil at one time the RfD (D1, 0.3 µg/g), and ten times the RfD (D10, 3 µg/g) (RfD = 100 g a.i. /ha, (ACTA- Les Instituts Techniques Agricoles, France, 2023)). Tubes were left open for 2 hours under a fume hood to evaporate the MeOH. Then, soil level was completed to reach the appropriate dry soil mass and tubes were shaken by inversion during 5 min to ensure a complete mixture of TBT in soil. Mixed and contaminated soils were then transferred into the microcosm boxes and sterile distilled water

was added on the top to reach 20 g of soil at 20% relative humidity (% dw) per microcosm. Microcosms were then lidded and incubated in the dark at 21 ± 2 °C. Sampling by sacrifice was done on the microcosms at 0 (+ 10 min after setup); 3; 7; 14; 25; 40 and 55 days after treatment. Every 2 days, microcosms were ventilated, and the soil moisture was adjusted if needed by addition of distilled water under sterile conditions. Soil microcosms were prepared in triplicates for each treatment and time points (n = 63).

2.3. Microbial community structure

2.3.1. DNA extraction, purification, and quantification

Soil microbial DNA extraction was performed on 0.250 g of soil immediately after sampling, using the ZymoBIOMICS™ DNA Miniprep Kit (Zymo Research, USA). DNA extracts were stored at -20°C until use. DNA quality was checked by migration of PCR products (amplification of the 16S rRNA gene) on agarose gel electrophoresis. DNA was quantified using the Quant-iT™ PicoGreen® dsDNA Assay Kit P7589 (Invitrogen™, France). A mean of 14.5 ± 1.7 µg/g of soil was obtained.

2.3.2. Amplicon sequencing

The diversity of total and *hppd*-containing bacterial communities was monitored by sequencing (Illumina MiSeq paired end sequencing, 2 x 300pb) 16S rRNA and *hppd* amplicons, respectively. *hppd* amplicon libraries were prepared from DNA extracts using a two-step PCR protocol described previously (Thiour-Mauprivez et al., 2020, 2021), with a PCR#1 volume of 3 µL instead of 1 µL used as template in PCR#2. 16S rRNA amplicons libraries were prepared from DNA extracts also with a two-step PCR protocol targeting the hypervariable *V3-V4* region using the 341F (5- CCTACGGGNGGCWGCAG- 3) and 805R (5- GACTACHVGGGTATCTAATCC- 3) primer pair (Klindworth et al., 2013). Preparation,

verification, and normalization of these libraries was performed by the Bio-Environment platform (University of Perpignan Via Domitia, France). Primer pairs contained, appended to 5' end, adaptor sequences followed by 2 or 3 random N bases used as spacers to add diversity in the Illumina flow cell cluster detection. 16S rRNA libraries and *hppd* libraries were pooled with proportion of 2/3 and 1/3 respectively and sequenced in only one Illumina flow cell by the Bio-Environment platform (University of Perpignan Via Domitia, France). All sequences were submitted to NCBI under the BioProject accession number PRJNA1011008.

2.3.3. Bioinformatic analysis of amplicon sequences

Analysis of *hppd* amplicon sequencing data was performed as described previously (Thiour-Mauprivez et al., 2021), with the difference that *hppd* amplicon sequences were clustered at 85% amino-acid sequence identity threshold after conversion of DNA sequences into protein sequences (HPPD clusters). Multiple sequence alignment of HPPD sequences identified by differential abundance analysis (see 3.3) and phylogenetic reconstructions were performed using the function "build" of ETE3 3.1.2 (Huerta-Cepas et al., 2016), as implemented on GenomeNet (https://www.genome.jp/tools/ete/). Phylogenetic tree of the aligned sequences was constructed using FastTree v2.1.8 default parameters (Price et al., 2010). Taxonomic affiliations of HPPD clusters were retrieved using NCBI's blastp against the nr database.

16S rRNA sequence data were analyzed using QIIME 2™ (Quantitative Insight into Microbial Ecology) version 2022.8.3 (Bolyen et al., 2019). Primers and heterogeneity spacers were removed from the reads with CUTADAPT (Martin, 2011). Reads were filtered, denoised, assembled and chimeras removed using the DADA2 plugin (Callahan et al., 2016) with default settings and trimmed at the 3' end of reads based on sequence quality scores (trimming at 280 bp for forward reads, 250 bp for reverse reads). Representative sequences for each Amplicon Sequence Variant (ASV) were aligned using MAFFT (Katoh & Standley, 2013) and

a 16S phylogenetic tree was constructed using FastTree (Price et al., 2010). Taxonomy was assigned to ASVs using the FEATURE CLASSIFIER plugin with a classifier previously trained on the 16S rRNA V3-V4 region (Bokulich et al., 2018). The SILVA 138 SSURef NR99 reference database pre-formatted with RESCRIPt was used to train the classifier (Quast et al., 2013; Robeson et al., 2021).

Alpha diversity indexes were calculated for HPPD clusters or ASV rarefied tables (subsampling by minimum depth). Principal Coordinate Analysis (PCoA) plots were generated (in QIIME for *hppd* and QIIME 2™ for 16S rRNA) based on weighted and unweighted UniFrac, Bray Curtis or Jaccard distance matrices to detect variations in the composition of communities and coordinates were used to create 3D figures using the EMPEROR plugin of QIIME 2™ (Vázquez-Baeza et al., 2013).

2.4. Tembotrione fate in soil microcosms

At each time point of the experiment, 10 g of soil were collected from microcosms and stored at -20°C for further TBT quantification as described below.

2.4.1. Herbicide extraction & chromatographic analysis

A modified QuEChERS (for Quick, Easy, Cheap, Efficient, Rugged and Safe) method from Rani and co-authors (Rani et al., 2020) was adapted to extract TBT from our soil samples. Briefly, 15 mL of DCM was added to the 10 g of soil in 50 mL conical polypropylene tubes. After 5 min of vortexing at maximum power followed by 5 min of ultrasonication at 37 kHz at room temperature and 20 min of mixing by inversion, samples were centrifuged at 4750xG for 10 min. Supernatants were carefully collected and a second extraction was done as previously described above. The two supernatants were combined, and DCM was evaporated to dryness at 30°C using a rotary evaporator. Dry extracts were resuspended in 2 mL of MeOH and stored

at -20°C prior to analysis. Extracts were analyzed by a High-Performance Liquid Chromatography (HPLC) VWR Hitachi LaChrom apparatus consisting in an auto-sampler L-2200, HTA L-2130 pump modules equipped with a Discovery® C18 column (5µm, 150 mm × 4.6 mm) and a DAD L-2450 UV/Vis detector set at λ=285 nm. For TBT detection, the mobile phase consisted in a mixture of water (AW) and acetonitrile (ACN) acidified with 0.1 % acetic acid, delivered at a flow rate of 1 mL/min under an isocratic mode 40/60 (AW/ACN) for 8 min.

2.4.2. Analytical performances

A calibration curve was obtained using blank soil sample replicates (n= 3) prepared according to the procedure mentioned above. Soil samples were spiked with a concentration range of TBT from 0.015 µg/g to 6 µg/g. Soil samples spiked only with MeOH were used to estimate matrix interferences. The mean recovery rate was estimated at 71 ± 5 % for TBT and the limit of quantification (LOQ) of the method was estimated at 0.1 µg/g, with a limit of detection (LOD) corresponding to ½ x LOQ = 0.05 µg/g. The obtained calibration curve (R^2 = 0.99) was used to estimate the concentration of TBT in microcosm soil extracts. Extraction and quantification steps were also performed for blank and MeOH control.

2.4.3. Fitting of dissipation models

Dissipation kinetics of TBT and endpoints were assessed following the recommendations of the FOCUS (Forum for the Co-ordination of pesticide fate models and their Use) Degradation Kinetics Workgroup (Boesten et al., 2006). Data points below the LOQ were removed and average values were used for each time point. A Fitting of the Single First Order (SFO) kinetic model was performed using the ModelMaker4 software. Dissipation Time 50 % (DT50) and error percentage of χ^2 test were calculated using the Excel spreadsheet provided by the FOCUS group (https://esdac.jrc.ec.europa.eu/projects/degradation-kinetics-software).

2.5. Statistical analysis

Differences in alpha diversity were analyzed with the R package v4.2.1 (R core team, 2022) using RStudio (2022.07.2). Homogeneity of variance (Levene's test) was checked prior to analysis of variance (ANOVA) and Tukey's honestly significant difference (HSD) tests. A significance threshold was set at a *p*-value of 0.05. Data were transformed and data points were removed when needed based on ANOVA results. Beta diversity distance matrices were subjected to a PERMANOVA analysis and pairwise tests.

A Generalized Linear Mixed effect Model (GLMM) analysis was performed to select discriminant HPPD clusters / ASVs between experimental treatments (Huet et al., 2023), using the function "glmer" from R package *lme4* (Bates et al., 2015) with a prior filtering of the HPPD clusters/ASVs based on their prevalence, relative abundance and headcount. Indeed, they were selected based on their presence in each triplicate (with relative abundance ≥ 0.0005) and with an average count ≥ 20 between triplicates within each treatment. A homemade script was used to identify the discriminant HPPD clusters/ASVs by performing an ANOVA on each of these HPPD clusters/ASVs.

3. Results

3.1. Effects of tembotrione on soil total bacterial community

The V3-V4 region of 16S rRNA genes was amplified from the soil DNA and sequenced to study the overall soil bacterial community structure and diversity. A range of 7713 to 36249

sequences per sample (mean = 22749 sequences) was obtained after a DADA2 analysis producing a feature table with 17324 ASVs. ASV table was rarefied at 7700 sequences.

Soil bacterial Beta diversity analysis (Figure 1) showed that the soil bacterial community composition was strongly affected by incubation time, as samples were visibly grouped according to time points on PCoA of weighted Unifrac distances, with significant differences (Pairwise PERMANOVA, $p = 0.001$). Beta diversity was not affected by any of the treatments applied to soil (Fig. 1).

Dominant phyla in the studied soil were *Actinobacteriota*, *Proteobacteria*, *Chloroflexi*, *Planctomycetota* and *Acidobacteria*, representing, when added together, approximately 80% in relative abundance, across all conditions (Figure S1). Even if variations occurred for less dominant phyla along the time course of the experiment (*i.e.,* increasing proportion of both *Verrucomicrobiota* and *Patescibacteria* from day 25 to 55), there were no visible changes in the taxonomic composition between treatments.

Richness, Faith's phylogenetic diversity (PD index), and evenness (Dominance) of 16S rRNA sequences were compared between treatments at each sampling time point (Table S1). Bacterial richness in soil, as measured by the Chao1 index, was influenced by sampling time and by TBT treatments too. Indeed, in control and D1 microcosms, level of richness dropped after day 3 before increasing above its initial level after day 14. In contrast, D10 microcosms stayed at their initial richness level from day 3 to day 14, before increasing at day 25 (Table S1). As a result, the mean richness was significantly higher in D10 microcosms than both control and D1 (Table 1). The evolution of the PD index among time and treatments showed a similar trend with average values significantly higher in D10 than in D1 and control microcosms (Table 1). The dominance index, estimating bacterial species evenness, showed important variations throughout the experiment span. Values were significantly lower in D10,

indicating a higher species evenness, compared to D1 and control (Table 1), this difference being most significant at day 3 (Table S1).

Overall, one can conclude that TBT applied at D1 had no significant effect on the diversity of the soil bacterial community. However, when applied at D10, TBT slightly increased richness and phylogenetic diversity in soils, even after 55 days post-treatment. At day 3, D10 TBT seems to limit the drop of specific evenness observed in control and D1 treatments.

3.2. Effect of tembotrione on soil *hppd*-containing bacterial community

hppd-amplicons were sequenced to assess the effect of TBT on *hppd*-soil bacterial community. A range of 6437 to 61138 sequences per sample (mean = 29162 sequences) remained after filtering and correction. The remaining sequences were grouped into 4667 clusters at 85% amino-acid sequence identity threshold. For further analysis, the obtained OTU table was rarefied at 6400 sequences.

Soil HPPD Beta diversity was investigated (Fig. 2). As previously, samples were grouped according to time points, independently of their treatment. Significant differences between time points were observed (Pairwise PEMANANOVA, $p = 0.001$), suggesting a strong effect of time on *hppd* bacterial community composition. However, community composition of soil HPPDs was not affected by TBT treatment.

Several alpha-diversity indexes were calculated to compare richness (observed clusters), PD index and evenness (Simpson's reciprocal) of HPPD clusters between treatments at each time point (Table S2). The average of the richness index showed that observed HPPD clusters were significantly lower in soil treated with the highest dose of TBT (Table 2). Compared to the control, a decrease ranging from 2.1 % to 7.3 % was observed between day 0 and day 40

(Table S2). A similar pattern was observed with the PD index of HPPD clusters which was significantly lower in D10 than in the control (Table 2) with a decrease of 0.8 to 5.5% from day 0 to day 40 (Table S2). Regarding Simpson's reciprocal index, no significant variation was observed between treatments (Table 2) although a trend was visible from day 3 to day 40 where values were lower in treated soils compared to control ones, but this was not statistically significant (Table S2).

Altogether, TBT applied at D1 does not impact neither the structure nor the composition of the *hppd*-containing bacterial community in soil microcosms. At the highest dose (D10), TBT slightly reduced richness and phylogenetic diversity of *hppd*-containing bacterial community in soil. These changes were nonetheless transient and did not persist until the end of the experiment.

3.3. Differential abundance analysis and identification of tembotrione-specific discriminating bacterial and *hppd*-containig taxa

To further investigate the impact of TBT treatment on ASVs and HPPD clusters in soils, a Generalized Linear Mixed effect Model (GLMM, glmer function, R package *lme4*) was performed on the most abundant and representative ASVs and HPPD clusters. Among the 963 ASVs analyzed and the 575 HPPD clusters, 26 ASVs from 16S rRNA data and 27 HPPD clusters were selected and identified as discriminant between different TBT treatments and/or within each time point (*p.adj*. < 0.05). They are listed in tables S3 and S4 with their corresponding taxonomic affiliations. The ASVs and HPPD clusters with the most relevant and significant variations in relative abundance were chosen for further analysis.

The mean fold change in relative abundance compared to controls, expressed in percentage, are shown for D1 and D10 at each day, for the selected and discriminating ASVs and HPPD clusters (Figures 3 and 4, respectively). Results showed that relative abundances were either enriched or reduced by TBT. Interestingly, there were discriminant bacterial ASVs and HPPD clusters sharing similar taxonomic affiliations and similar variations in relative abundance, such as the two Gammaproteobacteria *Steroidobacter* (ASV-60 and cluster-1573) and *Lysobacter* (ASV-425 and cluster-1463) and Alphaproteobacteria in the *Sphingomonadaceae* (ASV-365 and clusters-0 and cluster-1479).

Relative abundance of *Steroidobacter* (ASV-60, Fig. 3) and HPPD cluster affiliated to *Steroidobacter gossypii* (cluster-1573, Fig. 4) increased significantly at D10 (from 50% at day 3 to 70 % at day 7) compared to control. In both cases, after 7 days, control and treated soils showed similar relative abundances of these ASV/cluster. HPPD cluster-1553, also related to *S. gossypii*, showed similar results (data not shown).

Sequences affiliated to the *Lysobacter* genus were significantly reduced in treated soils during the experiment. This reduction was significant for ASV-425 at day 14 with a mean reduction of 30% to 40% (Fig. 3). This trend was clear for the HPPD cluster (*L. tabacisoli* cluster-1463) with significant reduction from day 7 to day 55 in both D1 and D10 and a greater effect for D10 with up to 50% reduction in relative abundance at day 7 (Fig. 4).

As for *Sphingomonadaceae*, two identified discriminant HPPD clusters associated with *Sphingomonas* sp. G124 (cluster-1479 and cluster-0) were enriched following TBT treatment in terms of relative abundance (Fig. 4). For cluster-1479 and cluster-0, significant increases (up to 60% and 20% compared to the control, respectively) occurred at day 3, 14, 25 (and day 40 for cluster-0) for D1 and D10. At day 55, the relative abundance of cluster-0 was significantly reduced in treated soils. Noteworthy, cluster-0 was the most abundant HPPD cluster found among all the *hppd* amplicon sequencing data, representing almost 10% of all

357 the HPPD clusters (data not shown). Other HPPD clusters affiliated to *Sphingomonas* showed
358 a similar but less clear trend (cluster-1564, cluster-1464, cluster-1470, data not shown). ASV-
359 365 (*Sphingomonadaceae,* genus *Sphingoaurantiacus*) shared similar variations with the
360 HPPD cluster-0 at the end of the experiment, with a significant decrease of its relative
361 abundance at day 40 and 55 in treated soils, but not as important as the one for the HPPD
362 clusters described above (Fig. 3).

363 Regarding *Betaproteobacteria*, three ASVs exhibited a significant decrease in relative
364 abundance in microcosms treated with TBT. ASV-21, assigned to the genus *Methylotenera*,
365 showed a relative abundance approximately 30% to 50% lower in D10 than in the control at
366 day 3, 7 and 14 (Fig. 3). ASV-568 and ASV-3, affiliated to the *Methylophilaceae* family (which
367 include the *Methylotenera* genus), exhibited similar variations (data not shown), unlike the
368 relative abundance of HPPD cluster 877 (*Massilia* spp.) which was significantly higher in
369 treated microcosms at day 3, 40 and 55 (Fig.4). Other HPPD clusters, associated with the
370 genus *Massilia*, also showed similar trends (cluster-728, 834, 123, 669, 1310 and 1304, data
371 not shown). Finally, the relative abundance of an HPPD sequence assigned to *Ramlibacter*
372 sp. WS9 (cluster-4101) exhibited a significant decrease at day 3 and 7 and an increase from
373 day 14 to 40 in the treated soils compared to the control ones (Fig. 4). A similar increase was
374 observed in another HPPD cluster also associated to *Ramlibacter* genus (cluster-4124) in D1
375 and D10 treatments at day 40 and 55 (data not shown).

376 Another interesting ASV, assigned to *Nitrospira* (*Nitrospirota;* ASV-29) decreased over time
377 with a significant drop in D10 microcosms at day 7 and 55 (approximately 40 % less abundant
378 than in the control, Fig. 3). ASV-193 (*Rhizobiaceae*, Alphaproteobacteria) was significantly
379 enriched in treated soils at day 3, with an increase of its relative abundance up to two-fold
380 compared to the control (Fig. 3).

381 Using the full HPPD sequences from the BLASTP best hit of each discriminant HPPD cluster
382 (see accession numbers on Table S4), a multiple sequence alignment allowed us to construct

a phylogenetic tree. Sequences from the clusters cited above but not shown in the figures were also included. Interestingly, the HPPD sequence from *Lysobacter tabacisoli* seems isolated and separated on a single branch of the tree, compared to other discriminant HPPD sequences (Fig. S2). Cluster-1463, which is affiliated to *Lysobacter tabacisoli*, is the only HPPD cluster negatively impacted by TBT treatment in soil, suggesting that the HPPD from this taxon might be sensitive to TBT, likely due to a specificity in its protein sequence.

To sum up, the results presented above indicate that, on the one hand, the proportions of *Steroidobacter*, *Sphingomonas*, *Massilia* and a taxon from the *Rhizobiaceae* family were enriched in TBT treated soils. *Lysobacter*, *Nitrospira* and *Methylotenera*, on the other hand, decreased in their relative abundance in the treated soils. These effects were identified through 16S rRNA or the *hppd* functional-gene marker, or both, for some taxa. Considering the D10 treatment, these effects seemed to be more significant, with some exceptions.

3.4. Tembotrione dissipation in soil microcosms

Aiming to assess the chemical behavior of the active ingredient during the exposure scenario of soil bacterial communities in microcosms and to better understand the effects observed on community composition, TBT concentration in soil microcosms was estimated at each time point, for both D1 and D10 TBT treatments. Expected concentrations of TBT were measured at the beginning of the experiment (day 0). A rapid dissipation of TBT was observed at D1 with concentration values reaching the LOD after 14 days (Figure 5B). At D10, TBT concentrations also decreased through time, reaching the RfD after 40 days. In this condition, TBT was still quantifiable at the end of the experiment (55 days) with an estimated concentration just above the LOD. Dissipation curves could reasonably fit a Single First Order (SFO) kinetic model ($C = C_0.e^{-kt}$), as estimated by error levels of chi2-tests, where values obtained were below 15% for the two doses applied (2.6% and 8.4% for D1 and D10, respectively ; fig. 5A). The half-life of TBT in soil microcosms was thus, estimated at 7 days for D1 and 15 days for D10.

To conclude, TBT was rapidly dissipated with an exponential decay in soil microcosms and TBT concentration was below the LOD after 14 days for D1 and just above the LOD after 55 days of incubation for D10.

4. Discussion

4.1. Effect of RfD of tembotrione on the structure of total and *hppd*-containing bacterial communities

Amplicon Illumina sequencing was used to determine the effect of TBT RfD on the diversity of the total- and on the *hppd*-containing bacterial communities. Our results suggest that, under our experimental conditions, TBT had no or a very little effect on the structure and the diversity of both the total- and the *hppd*-containing communities when applied at RfD (D1). This conclusion is consistent with what has already been observed, using a similar approach as ours, for other synthetic β-triketones herbicides applied at RfD in soil. Indeed, RfD of sulcotrione (active ingredient or formulated product) did not change soil bacterial and *hppd*-bacterial community composition and diversity (Romdhane et al., 2016; Thiour-Mauprivez et al., 2021), nor did RfD of mesotrione alone or formulated on the composition and diversity of total bacterial and nitrogen cycling bacterial communities in soil (Crouzet et al., 2010, 2016; Joly et al., 2012). These results could be explained by the low persistence of β-triketone herbicides in soil when applied at the RfD (*i.e.,*100 g/ha for TBT).

The studied soil has already been used in previous studies for DT_{50} determination of other β-triketones herbicides (*i.e.*, synthetic ones: sulcotrione, mesotrione or natural one: leptospermone,) with values ranging from 4 to 8 days when applied at RfD (Calvayrac et al., 2012; Chaabane et al., 2008; Romdhane, et al., 2016, 2019; Thiour-Mauprivez et al., 2021).

In some of these studies, high dissipation times were observed in abiotic controls, suggesting that herbicide degradation was mainly due to biological activity. From these living soils, several triketone-degrading bacterial strains were isolated (Batisson et al., 2009; Calvayrac et al., 2012; Chaabane et al., 2008; Romdhane, et al., 2016). The TBT dissipation kinetics observed in our experiments are in accordance with those found by Rani and co-authors (Rani et al., 2020), showing that dissipation of TBT applied at 0.12 µg/g in a sandy loam soil and a clayey loam soil followed first order kinetics with DT_{50} of 9.3 days and 8.1 days respectively. Also, other DT_{50} were estimated between 4 and 72 days (depending on soils physico-chemical characteristics) in soils maintained under aerobic conditions (EFSA, 2013; Tarara et al., 2009; US EPA, 2007). Thus, we can assume that, in soil microcosms treated with D1, TBT is rapidly dissipated, mostly due to its rapid biodegradation and, therefore, exposition of soil microorganisms to TBT is only occurring over a short period of time.

Romdhane et al. (Romdhane et al., 2016, 2019) showed that leptospermone, a triketone from natural origin, applied at the RfD had significant effects on the composition of soil bacterial communities. However, the authors highlighted the higher (~ 10-fold) application rate of leptospermone compared to synthetic β-triketones (i.e., 1500 g a.i. /ha for RfD).

4.2. Changes in bacterial and *hppd*-contaning communities to tembotrione exposition considering a higher exposure scenario

At the highest dose (D10), TBT had some ecotoxicological effects towards total- and *hppd*-bacterial communities. While overall community composition was not significantly affected, small but significant variations occurred in alpha-diversity measurements, driven by taxa with lower relative abundance. This is consistent with the exposure scenario, as the measured DT_{50}

was two times higher for D10 than that for D1. One could observe that, in D10 microcosms, TBT concentration was still three times the RfD 25 days after its application.

Total bacterial richness and phylogenetic diversity fluctuated over time but overall, and even when effect of sampling time was considered, they showed higher levels in D10 treated soils than in the control ones. This might be the result of the expansion of TBT-resistant bacterial populations and/or the growth of saprophytic bacterial species feeding on dead TBT-sensitive organisms, as previously suggested by Dumas and coworkers to explain the stimulation of heterotrophic communities in soil by high doses of pure or formulated mesotrione (Dumas et al., 2017). TBT-tolerant populations, rare or in low numbers before TBT application, are no longer in competition for resources with TBT-sensitives microorganisms and can colonize their niche. Moreover, TBT application might have favored the emergence of degrading-bacterial populations able to use TBT as an energy source. Indeed, several triketones degrading bacterial strains have been isolated from soils and the degradation pathway were identified for mesotrione and sulcotrione (Batisson et al., 2009; Calvayrac et al., 2012). Even if no TBT degrading soil strain has been isolated yet, we could hypothesize that they are present in our soil. Nguyen and co-authors (Nguyen et al., 2016), suggested, in a meta-analysis, that glyphosate at high doses of application could stimulate microbial growth, acting as a carbon, nitrogen, or phosphorus source. While the degrading community being promoted, one is then unable to detect the possible toxic effects on the sensitive community.

Meanwhile, D10 treatment decreased richness and phylogenetic diversity of HPPD clusters indicating a possible direct toxic effect on sensitive *hppd*-containing populations through a disruption of the tyrosine catabolic pathway *via* HPPD inhibition. This effect appeared to be transient and dependent on TBT presence in soil, as this effect was clearly visible until day 40 but not anymore at the end of the experiment, when TBT reached the LOD level.

These discrepancies between *hppd* and 16S rRNA gene amplicon analysis could likely be explained by the fact that the *hppd*-containing bacteria constitute a sub-pool of the total bacterial community containing the TBT targeted enzyme. Analysis of the total bacterial community mostly highlighted positive effects (Yang effect, *cf.* Karpouzaz et al., 2016) discussed above, thus hiding effects (Yin effects) seen on sensitive bacterial HPPD. This underlines the importance of looking at specific bacterial functional groups, in addition to taxonomic diversity, as conclusions on the effect of a pollutant on bacterial populations can be different, as our results show.

Finally, as our results showed that effect of TBT could occur in a worst-case scenario of exposure in controlled conditions, it would have been interesting to also test TBT effects in field experiments with more realistic exposure scenarios, but experimental conditions become difficult to control (Thiour-Mauprivez et al., 2021).

4.3. Taxa responding to TBT in soils: towards a new class of exposure biomarkers?

Since the relative abundance of some specific 16S rRNA ASVs and HPPD clusters was significantly influenced by TBT in the tested soil and that these ASVs and clusters shared the same or close taxonomic affiliations associated with the same responses, they could potentially represent HPPD+ bacterial taxa indicator of TBT or other β-triketones exposure in soil.

This was the case for *Sphingomonas* and *Steroidobacter*, whose relative abundances were increased by TBT. These taxa could use TBT as a carbon or energy source and/or could exhibit degradation capabilities. These taxa were also enriched in soils after leptospermone exposition (Romdhane et al., 2016; 2019) and the degradation of other herbicides in soil such as isoproturon, 2,4-D or fomesafen by *Sphingomonas* has already been shown (Hu et al.,

2019; Sørensen et al., 2001; Vanitha et al., 2023). The genus *Steroidobacter* is known to be associated with the rhizosphere of diverse plants and has a range of organic compound-degrading capabilities (Gong et al., 2016; Ikenaga et al., 2021). Moreover, taxa from the same genera could have benefited from resources left by sensitive populations in the community and might be tolerant to TBT or even harbor resistant HPPDs, as it was the case for a *Sphingobium* strain, a Sphingomonadales genus phylogenetically close to *Sphingomonas* species, that possesses an HPPD resistant to mesotrione and TBT to a lesser extent (Liu et al., 2020).

Other 16S rRNA ASVs and HPPD clusters enriched in TBT treated soils are associated to species that are known to (i) degrade herbicides or other organic compounds: linuron and polycyclic aromatic carbons for *Ramlibacter* (Lerner et al., 2020; Su et al., 2022), chloroacetamide and atrazine in soil for *Massilia* (Lee et al., 2017; Luo et al., 2021) ; (ii) be involved in plant-bacteria symbiosis and are able to degrade complex organic molecules for members of the *Rhizobiaceae* family (Carrareto Alves et al., 2014).

Conversely, 16S rRNA ASV and HPPD cluster associated to *Lysobacter* were negatively affected by TBT, indicating a potential sensitivity of their HPPD. To our knowledge, no previous study has investigated HPPD sensitivity to β-triketones in *Lysobacter*. Interestingly, the alignment and phylogenetic analysis of HPPD sequences showed that *Lysobacter* HPPD has an amino acid sequence distinct from the other taxa. In addition, as far as we know, no previous study reported negative effects of PPP on this taxon in soil. However, it has already been observed that members of this genus have degrading abilities and are promoted by the use of acetochlor S, an herbicide, in soil (Han et al., 2021). Nonetheless, negative effects of TBT on *Lysobacter* could be of ecological importance as this genus is recognized as a beneficial organism in the rhizosphere and acts as a protective agent against some plant pathogens (Brescia et al., 2020; Huang et al., 2022).

Similarly, the relative abundance of *Nitrospira* was significantly reduced by TBT, similarly to previous observations after exposition to the herbicide linuron in soil (Medo et al., 2021). *Nitrospira* is found in rhizospheric habitats and is involved in the nitrogen cycle (Daims & Wagner, 2018) so, a potential toxicity of herbicides on this strain could then be of ecological importance. It should be noticed that this genus is known to possess an HPPD but, it was absent from our *hppd* sequencing dataset. It was also the case for *Methylotenera* ASVs, which were decreased in TBT-treated soil and which might play a role in the nitrogen cycle too (Yi et al. 2022). This taxon is not known to possess the *hppd* gene so its TBT-sensitivity could not be explained by a toxic action of TBT on its HPPD.

We hence suggest a use of the TBT-sensitive taxa identified in our study, notably those carrying an HPPD and negatively affected, or their respective *hppd* genes, as potential biomarkers of exposure to triketones in soils.

5. Conclusion

To our knowledge, this is the first study to assess the fate and ecotoxicological impacts of TBT herbicide on soil microbial communities. Our results showed that the active ingredient applied in microcosms according to field recommendations did not have a significant impact, neither on the structure of soil microbial community, nor on the structure of non-targeted bacterial *hppd* community. However, TBT applied at tenfold the RfD might negatively affect some sensitive populations, even though these effects were light and could have been hidden by the emergence and selection of tolerant and/or degrading populations within the soil bacterial community. This was supported by an easy and rapid dissipation of the active ingredient in soil. Thus, both enhanced bacterial taxa with putative TBT-degrading abilities and/or TBT-tolerance and diminished taxa with potential sensitive HPPD, identified by our differential

abundance analysis, could be proposed in ERA as relevant biomarkers of TBT-contaminated agricultural soils.

6. Acknowledgments

The authors thank the Région Occitanie, and Perpignan University Via Domitia for their financial support, and Laetitia Fournier for her technical help.

7. Funding

This work was supported by the Région Occitanie and Université de Perpignan Via Domitia

8. References

ACTA- Les Instituts Techniques Agricoles. (2023). Index acta phytosanitaire 2021, 59ème édition (Acta éditions, Vol. 59).

Bates, D., Mächler, M., Bolker, B. M., & Walker, S. C. (2015). Fitting Linear Mixed-Effects Models Using lme4. Journal of Statistical Software, 67(1), 1–48. https://doi.org/10.18637/JSS.V067.I01

Batisson, I., Crouzet, O., Besse-Hoggan, P., Sancelme, M., Mangot, J. F., Mallet, C., & Bohatier, J. (2009). Isolation and characterization of mesotrione-degrading Bacillus sp. from soil. Environmental Pollution, 157(4), 1195–1201. https://doi.org/10.1016/j.envpol.2008.12.009

571 Boesten, J. J. T. I., Aden, K., Beigel, C., Beulke, S., Dust, M., Dyson, J. S., Fomsgaard, S.,
572 Jones, R. L., Karlsson, S., Van Der Linden, A. M. A., Richter, O., Magrans, J. O., & Soulas,
573 G. (2006). Guidance Document on Estimating Persistence and Degradation Kinetics from
574 Environmental Fate Studies on Pesticides in EU Registration The Final Report of the Work
575 Group on Degradation Kinetics of FOCUS (FOrum for the Co-ordination of pesticide fate
576 models and their USe).

577 Bokulich, N. A., Kaehler, B. D., Rideout, J. R., Dillon, M., Bolyen, E., Knight, R., Huttley, G.
578 A., & Gregory Caporaso, J. (2018). Optimizing taxonomic classification of marker-gene
579 amplicon sequences with QIIME 2's q2-feature-classifier plugin. Microbiome, 6(1), 1–17.
580 https://doi.org/10.1186/S40168-018-0470-Z/TABLES/3

581 Bolyen, E., Rideout, J. R., Dillon, M. R., Bokulich, N. A., Abnet, C. C., Al-Ghalith, G. A.,
582 Alexander, H., Alm, E. J., Arumugam, M., Asnicar, F., Bai, Y., Bisanz, J. E., Bittinger, K.,
583 Brejnrod, A., Brislawn, C. J., Brown, C. T., Callahan, B. J., Caraballo-Rodríguez, A. M.,
584 Chase, J., … Caporaso, J. G. (2019). Reproducible, interactive, scalable and extensible
585 microbiome data science using QIIME 2. Nature Biotechnology, 37(8), 852–857.
586 https://doi.org/10.1038/S41587-019-0209-9

587 Borowik, A., Wyszkowska, J., Kucharski, J., Baćmaga, M., & Tomkiel, M. (2017). Response
588 of microorganisms and enzymes to soil contamination with a mixture of terbuthylazine,
589 mesotrione, and S-metolachlor. Environmental Science and Pollution Research, 24(2),
590 1910–1925. https://doi.org/10.1007/s11356-016-7919-z

591 Brescia, F., Pertot, I., & Puopolo, G. (2020). Lysobacter. In Beneficial Microbes in Agro-
592 Ecology: Bacteria and Fungi (pp. 313–338). Elsevier. https://doi.org/10.1016/B978-0-12-
593 823414-3.00016-2

Callahan, B. J., McMurdie, P. J., Rosen, M. J., Han, A. W., Johnson, A. J. A., & Holmes, S. P. (2016). DADA2: High resolution sample inference from Illumina amplicon data. Nature Methods, 13(7), 581. https://doi.org/10.1038/NMETH.3869

Calvayrac, C., Martin-Laurent, F., Faveaux, A., Picault, N., Panaud, O., Coste, C. M., Chaabane, H., & Cooper, J. F. (2012). Isolation and characterisation of a bacterial strain degrading the herbicide sulcotrione from an agricultural soil. Pest Management Science, 68(3), 340–347. https://doi.org/10.1002/PS.2263

Carrareto Alves, L. M., De Souza, J. A. M., Varani, A. D. M., & Lemos, E. G. D. M. (2014). The family Rhizobiaceae. The Prokaryotes: Alphaproteobacteria and Betaproteobacteria, 9783642301971, 419–437. https://doi.org/10.1007/978-3-642-30197-1_297/COVER

Cébron, A., Karpouzas, D. G., Martin-Laurent, F., Morin, S., Palacios, C., & Schmitt-Jansen, M. (2022). Editorial: Microbial Ecotoxicology Advances to Improve Environmental and Human Health Under Global Change. *Frontiers in Microbiology*, *13*, 870404. https://doi.org/10.3389/FMICB.2022.870404/BIBTEX

Chaabane, H., Vulliet, E., Calvayrac, C., Coste, C. M., & Cooper, J. F. (2008). Behaviour of sulcotrione and mesotrione in two soils. Pest Management Science, 64(1), 86–93. https://doi.org/10.1002/PS.1456

Crouzet, O., Batisson, I., Besse-Hoggan, P., Bonnemoy, F., Bardot, C., Poly, F., Bohatier, J., & Mallet, C. (2010). Response of soil microbial communities to the herbicide mesotrione: A dose-effect microcosm approach. Soil Biology and Biochemistry, 42(2), 193–202. https://doi.org/10.1016/j.soilbio.2009.10.016

Crouzet, O., Wiszniowski, J., Donnadieu, F., Bonnemoy, F., Bohatier, J., & Mallet, C. (2013). Dose-dependent effects of the herbicide mesotrione on soil cyanobacterial communities.

Archives of Environmental Contamination and Toxicology, *64*(1), 23–31. https://doi.org/10.1007/s00244-012-9809-9

Crouzet, O., Poly, F., Bonnemoy, F., Bru, D., Batisson, I., Bohatier, J., Philippot, L., & Mallet, C. (2016). Functional and structural responses of soil N-cycling microbial communities to the herbicide mesotrione: a dose-effect microcosm approach. Environmental Science and Pollution Research, 23(5), 4207–4217. https://doi.org/10.1007/S11356-015-4797-8/METRICS

Daims, H., & Wagner, M. (2018). Nitrospira. Trends in Microbiology, 26(5), 462–463. https://doi.org/10.1016/J.TIM.2018.02.001

Du, Z., Zhu, Y., Zhu, L., Zhang, J., Li, B., Wang, J., Wang, J., Zhang, C., & Cheng, C. (2018). Effects of the herbicide mesotrione on soil enzyme activity and microbial communities. Ecotoxicology and Environmental Safety, 164(April), 571–578. https://doi.org/10.1016/j.ecoenv.2018.08.075

Dumas, E., Giraudo, M., Goujon, E., Halma, M., Knhili, E., Stauffert, M., Batisson, I., Besse-Hoggan, P., Bohatier, J., Bouchard, P., Celle-Jeanton, H., Costa Gomes, M., Delbac, F., Forano, C., Goupil, P., Guix, N., Husson, P., Ledoigt, G., Mallet, C., … Sarraute, S. (2017). Fate and ecotoxicological impact of new generation herbicides from the triketone family: An overview to assess the environmental risks. Journal of Hazardous Materials, 325, 136–156. https://doi.org/10.1016/j.jhazmat.2016.11.059

EFSA (2013). Conclusion on the peer review of the pesticide risk assessment of the active substance tembotrione. EFSA Journal, 11(3), 1–81. https://doi.org/10.2903/j.efsa.2013.3131

Gong, Z. L., Zhang, C. F., Jin, R., & Zhang, Y. Q. (2016). Steroidobacter flavus sp. nov., a microcystin-degrading Gammaproteobacterium isolated from soil. Antonie van Leeuwenhoek, 109(8), 1073–1079. https://doi.org/10.1007/S10482-016-0706-5

641 Griffiths, B. S., & Philippot, L. (2013). Insights into the resistance and resilience of the soil
642 microbial community. *FEMS Microbiology Reviews*, *37*(2), 112–129.
643 https://doi.org/10.1111/J.1574-6976.2012.00343.X

644 Han, L., Fang, K., Liu, Y., Fang, J., Wang, F., & Wang, X. (2021). Earthworms accelerated
645 the degradation of the highly toxic acetochlor S-enantiomer by stimulating soil microbiota in
646 repeatedly treated soils. *Journal of Hazardous Materials*, *420*, 126669.
647 https://doi.org/10.1016/j.jhazmat.2021.126669

648 Huerta-Cepas, J., Serra, F., & Bork, P. (2016). ETE 3: Reconstruction, Analysis, and
649 Visualization of Phylogenomic Data. *Molecular Biology and Evolution*, *33*(6), 1635–1638.
650 https://doi.org/10.1093/MOLBEV/MSW046

651 Hicks, L. C., Frey, B., Kjøller, R., Lukac, M., Moora, M., Weedon, J. T., & Rousk, J. (2022).
652 Toward a function-first framework to make soil microbial ecology predictive. *Ecology*, *103*(2),
653 e03594. https://doi.org/10.1002/ECY.3594

654 Hu, H., Zhou, H., Zhou, S., Li, Z., Wei, C., Yu, Y., & Hay, A. G. (2019). Fomesafen impacts
655 bacterial communities and enzyme activities in the rhizosphere. Environmental Pollution,
656 253, 302–311. https://doi.org/10.1016/J.ENVPOL.2019.07.018

657 Huet, S., Romdhane, S., Breuil, M.-C., Bru, D., Mounier, A., Spor, A., & Philippot, L. (2023).
658 Experimental community coalescence sheds light on microbial interactions in soil and
659 restores impaired functions. *Microbiome*, *11*(1), 42. https://doi.org/10.1186/s40168-023-
660 01480-7

661 Huang, X., Yang, X., Lin, J., Franks, A. E., Cheng, J., Zhu, Y., Shi, J., Xu, J., Yuan, M., Fu,
662 X., & He, Y. (2022). Biochar alleviated the toxicity of atrazine to soybeans, as revealed by
663 soil microbial community and the assembly process. Science of The Total Environment, 834,
664 155261. https://doi.org/10.1016/J.SCITOTENV.2022.155261

665 Ikenaga, M., Kataoka, M., Yin, X., Murouchi, A., & Sakai, M. (2021). Characterization and
666 Distribution of Agar-degrading Steroidobacter agaridevorans sp. nov., Isolated from
667 Rhizosphere Soils. Microbes and Environments, 36(1).
668 https://doi.org/10.1264/JSME2.ME20136

669 Joly, P., Besse-Hoggan, P., Bonnemoy, F., Batisson, I., Bohatier, J., & Mallet, C. (2012).
670 Impact of Maize Formulated Herbicides Mesotrione and S-Metolachlor, Applied Alone and in
671 Mixture, on Soil Microbial Communities. ISRN Ecology, 2012, 1–9.
672 https://doi.org/10.5402/2012/329898

673 Joly, P., Bonnemoy, F., Charvy, J. C., Bohatier, J., & Mallet, C. (2013). Toxicity assessment
674 of the maize herbicides S-metolachlor, benoxacor, mesotrione and nicosulfuron, and their
675 corresponding commercial formulations, alone and in mixtures, using the Microtox® test.
676 Chemosphere, 93(10), 2444–2450. https://doi.org/10.1016/j.chemosphere.2013.08.074

677 Joly, P., Misson, B., Perrière, F., Bonnemoy, F., Joly, M., Donnadieu-Bernard, F., Aguer, J.
678 P., Bohatier, J., & Mallet, C. (2014). Soil surface colonization by phototrophic indigenous
679 organisms, in two contrasted soils treated by formulated maize herbicide mixtures.
680 *Ecotoxicology*, *23*(9), 1648–1658. https://doi.org/10.1007/s10646-014-1304-9

681 Kaczynski, P., Lozowicka, B., Hrynko, I., & Wolejko, E. (2016). Behaviour of mesotrione in
682 maize and soil system and its influence on soil dehydrogenase activity. Science of the Total
683 Environment, 571, 1079–1088. https://doi.org/10.1016/j.scitotenv.2016.07.100

684 Karpouzas, D. G., Tsiamis, G., Trevisan, M., Ferrari, F., Malandain, C., Sibourg, O., &
685 Martin-Laurent, F. (2016). ”LOVE TO HATE” pesticides: felicity or curse for the soil microbial
686 community? An FP7 IAPP Marie Curie project aiming to establish tools for the assessment
687 of the mechanisms controlling the interactions of pesticides with soil microorganisms.

688 *Environmental Science and Pollution Research*, *23*(18), 18947–18951.
689 https://doi.org/10.1007/S11356-016-7319-4/METRICS

690 Katoh, K., & Standley, D. M. (2013). MAFFT Multiple Sequence Alignment Software Version
691 7: Improvements in Performance and Usability. Molecular Biology and Evolution, 30(4), 772–
692 780. https://doi.org/10.1093/MOLBEV/MST010

693 Klindworth, A., Pruesse, E., Schweer, T., Peplies, J., Quast, C., Horn, M., & Glöckner, F. O.
694 (2013). Evaluation of general 16S ribosomal RNA gene PCR primers for classical and next-
695 generation sequencing-based diversity studies. Nucleic Acids Research, 41(1).
696 https://doi.org/10.1093/NAR/GKS808

697 Lee, H., Kim, D. U., Park, S., Yoon, J. H., & Ka, J. O. (2017). Massilia chloroacetimidivorans
698 sp. nov., a chloroacetamide herbicide-degrading bacterium isolated from soil. Antonie van
699 Leeuwenhoek, 110(6), 751–758. https://doi.org/10.1007/S10482-017-0845-3

700 Lerner, H., Öztürk, B., Dohrmann, A. B., Thomas, J., Marchal, K., De Mot, R., Dehaen, W.,
701 Tebbe, C. C., & Springael, D. (2020). Culture-Independent Analysis of Linuron-Mineralizing
702 Microbiota and Functions in on-Farm Biopurification Systems via DNA-Stable Isotope
703 Probing: Comparison with Enrichment Culture. Environmental Science and Technology,
704 54(15), 9387–9397.
705 https://doi.org/10.1021/ACS.EST.0C02124/SUPPL_FILE/ES0C02124_SI_002.XLSX

706 Liu, B., Peng, Q., Sheng, M., Ni, H., Xiao, X., Tao, Q., He, Q., & He, J. (2020). Isolation and
707 Characterization of a Topramezone-Resistant 4-Hydroxyphenylpyruvate Dioxygenase from
708 Sphingobium sp. TPM-19. Journal of Agricultural and Food Chemistry, 68(4), 1022–1029.
709 https://doi.org/10.1021/ACS.JAFC.9B06871/SUPPL_FILE/JF9B06871_SI_001.PDF

710 Luo, S., Zhen, Z., Zhu, X., Ren, L., Wu, W., Zhang, W., Chen, Y., Zhang, D., Song, Z., Lin,
711 Z., & Liang, Y. Q. (2021). Accelerated atrazine degradation and altered metabolic pathways

712 in goat manure assisted soil bioremediation. Ecotoxicology and Environmental Safety, 221.
713 https://doi.org/10.1016/J.ECOENV.2021.112432

714 Mamy, L. (ed.), Pesce, S. (ed.), Sanchez, W. (ed.), Leenhardt, S. (ed.), Amichot, M.,
715 Artigas, J., Aviron, S., Barthélémy, C., Beaudouin, R., Bedos, C., Berard, A., Berny, P.,
716 Bertrand, C., Bertrand, C., Betoulle, S., Bureau-Point, E., Charles, S., Chaumot, A., Chauvel,
717 B., … Tournebize, J. (2022). *Impacts des produits phytopharmaceutiques sur la biodiversité*
718 *et les services écosystémiques. Rapport d'ESCo*. https://doi.org/10.17180/0GP2-CD65

719 Martin, M. (2011). Cutadapt removes adapter sequences from high-throughput sequencing
720 reads. EMBnet.Journal, 17(1), 10–12. https://doi.org/10.14806/EJ.17.1.200

721 Medo, J., Maková, J., Medová, J., Lipková, N., Cinkocki, R., Omelka, R., & Javoreková, S.
722 (2021). Changes in soil microbial community and activity caused by application of
723 dimethachlor and linuron. Scientific Reports, 11(1), 12786. https://doi.org/10.1038/S41598-
724 021-91755-6

725 Moran, G. R. (2005). 4-Hydroxyphenylpyruvate dioxygenase. *Archives of Biochemistry and*
726 *Biophysics*, *433*(1), 117–128. https://doi.org/10.1016/J.ABB.2004.08.015

727 Nguyen, D. B., Rose, M. T., Rose, T. J., Morris, S. G., & van Zwieten, L. (2016). Impact of
728 glyphosate on soil microbial biomass and respiration: A meta-analysis. Soil Biology and
729 Biochemistry, 92, 50–57. https://doi.org/10.1016/J.SOILBIO.2015.09.014

730 Pavan, M. E., López, N. I., & Pettinari, M. J. (2020). Melanin biosynthesis in bacteria,
731 regulation and production perspectives. Applied Microbiology and Biotechnology, 104(4),
732 1357–1370. https://doi.org/10.1007/s00253-019-10245-y

733 Petric, I., Karpouzas, D. G., Bru, D., Udikovic-Kolic, N., Kandeler, E., Djuric, S., & Martin-
734 Laurent, F. (2016). Nicosulfuron application in agricultural soils drives the selection towards
735 NS-tolerant microorganisms harboring various levels of sensitivity to nicosulfuron.

Environmental Science and Pollution Research, *23*(5), 4320–4333. https://doi.org/10.1007/s11356-015-5645-6

Pose-Juan, E., Sánchez-Martín, M. J., Herrero-Hernández, E., & Rodríguez-Cruz, M. S. (2015). Application of mesotrione at different doses in an amended soil: Dissipation and effect on the soil microbial biomass and activity. Science of the Total Environment, 536, 31–38. https://doi.org/10.1016/j.scitotenv.2015.07.039

Price, M. N., Dehal, P. S., & Arkin, A. P. (2010). FastTree 2 – Approximately Maximum-Likelihood Trees for Large Alignments. PLOS ONE, 5(3), e9490. https://doi.org/10.1371/JOURNAL.PONE.0009490

Puglisi, E. (2017). Response of microbial organisms (aquatic and terrestrial) to pesticides. EFSA Supporting Publications, 9(11). https://doi.org/10.2903/sp.efsa.2012.en-359

Quast, C., Pruesse, E., Yilmaz, P., Gerken, J., Schweer, T., Yarza, P., Peplies, J., & Glöckner, F. O. (2013). The SILVA ribosomal RNA gene database project: improved data processing and web-based tools. Nucleic Acids Research, 41(Database issue). https://doi.org/10.1093/NAR/GKS1219

Rani, N., Duhan, A., & Tomar, D. (2020). Ultimate fate of herbicide tembotrione and its metabolite TCMBA in soil. Ecotoxicology and Environmental Safety, 203(July), 111023. https://doi.org/10.1016/j.ecoenv.2020.111023

Robeson, M. S., O'Rourke, D. R., Kaehler, B. D., Ziemski, M., Dillon, M. R., Foster, J. T., & Bokulich, N. A. (2021). RESCRIPt: Reproducible sequence taxonomy reference database management. PLOS Computational Biology, 17(11), e1009581. https://doi.org/10.1371/JOURNAL.PCBI.1009581

Romdhane, S., Devers-Lamrani, M., Barthelmebs, L., Calvayrac, C., Bertrand, C., Cooper, J. F., Dayan, F. E., & Martin-Laurent, F. (2016). Ecotoxicological impact of the bioherbicide

760 leptospermone on the microbial community of two arable soils. Frontiers in Microbiology,
761 7(MAY), 1–12. https://doi.org/10.3389/fmicb.2016.00775

762 Romdhane, S., Devers-Lamrani, M., Beguet, J., Bertrand, C., Calvayrac, C., Salvia, M. V.,
763 Jrad, A. Ben, Dayan, F. E., Spor, A., Barthelmebs, L., & Martin-Laurent, F. (2019).
764 Assessment of the ecotoxicological impact of natural and synthetic β-triketone herbicides on
765 the diversity and activity of the soil bacterial community using omic approaches. Science of
766 the Total Environment, 651, 241–249. https://doi.org/10.1016/j.scitotenv.2018.09.159

767 Singh, D., Kumar, J., & Kumar, A. (2018). Isolation of pyomelanin from bacteria and
768 evidences showing its synthesis by 4-hydroxyphenylpyruvate dioxygenase enzyme encoded
769 by hppD gene. *International Journal of Biological Macromolecules*, *119*, 864–873.
770 https://doi.org/10.1016/J.IJBIOMAC.2018.08.003

771 Sørensen, S. R., Ronen, Z., & Aamand, J. (2001). Isolation from Agricultural Soil and
772 Characterization of a Sphingomonas sp. Able To Mineralize the Phenylurea Herbicide
773 Isoproturon. Applied and Environmental Microbiology, 67(12), 5403.
774 https://doi.org/10.1128/AEM.67.12.5403-5409.2001

775 Su, A., Xu, Y., Xu, M., Ding, S., Li, M., & Zhang, Y. (2022). Resilience of the wheat root-
776 associated microbiome to the disturbance of phenanthrene. The Science of the Total
777 Environment, 838(Pt 3). https://doi.org/10.1016/J.SCITOTENV.2022.156487

778 Vanitha, T. K., Suresh, G., Mohan Bhandi, M., Krishna Reddy Mudiam, M., & Mohan, S. V.
779 (2023). Microbial Degradation of Organochlorine Pesticide: 2,4-Dichlorophenoxyacetic acid
780 by Axenic and Mixed Consortium. Bioresource Technology, 129031.
781 https://doi.org/10.1016/J.BIORTECH.2023.129031

782 Tarara, G., Fliege, R., Desmarteau, D., Kley, C., & Peters, B. (2009). Environmental fate of
783 tembotrione. *Bayer CropScience Journal*, *62*, 63-78.

784 Tawk, A., Deborde, M., Labanowski, J., & Gallard, H. (2015). Chlorination of the β-triketone
785 herbicides tembotrione and sulcotrione: Kinetic and mechanistic study, transformation
786 products identification and toxicity. *Water Research*, *76*, 132–142.
787 https://doi.org/10.1016/j.watres.2015.02.060

788 Thiour-Mauprivez, C., Martin-Laurent, F., Calvayrac, C., & Barthelmebs, L. (2019). Effects of
789 herbicide on non-target microorganisms: Towards a new class of biomarkers? *Science of the*
790 *Total Environment*, *684*, 314–325. https://doi.org/10.1016/j.scitotenv.2019.05.230

791 Thiour-Mauprivez, C., Devers-Lamrani, M., Mounier, A., Beguet, J., Spor, A., Calvayrac, C.,
792 Barthelmebs, L., & Martin-Laurent, F. (2020). Design of a degenerate primer pair to target a
793 bacterial functional community: The hppd bacterial gene coding for the enzyme targeted by
794 herbicides, a study case. Journal of Microbiological Methods, 170(January), 105839.
795 https://doi.org/10.1016/j.mimet.2020.105839

796 Thiour-Mauprivez, C., Devers-Lamrani, M., Bru, D., Béguet, J., Spor, A., Mounier, A., Alletto,
797 L., Calvayrac, C., Barthelmebs, L., & Martin-Laurent, F. (2021). Assessing the Effects of β-
798 Triketone Herbicides on the Soil Bacterial and hppd Communities: A Lab-to-Field
799 Experiment. Frontiers in Microbiology, 11, 1–10. https://doi.org/10.3389/fmicb.2020.610298

800 Thiour-Mauprivez, C., Dayan, F. E., Terol, H., Devers, M., Calvayrac, C., Martin-Laurent, F.,
801 & Barthelmebs, L. (2022). Assessing the effects of β-triketone herbicides on HPPD from
802 environmental bacteria using a combination of in silico and microbiological approaches.
803 Environmental Science and Pollution Research. https://doi.org/10.1007/s11356-022-22801-7

804 Vázquez-Baeza, Y., Pirrung, M., Gonzalez, A., & Knight, R. (2013). EMPeror: a tool for
805 visualizing high-throughput microbial community data. GigaScience, 2(1).
806 https://doi.org/10.1186/2047-217X-2-16

Yi, M., Zhang, L., Qin, C., Lu, P., Bai, H., Han, X., & Yuan, S. (2022). Temporal changes of microbial community structure and nitrogen cycling processes during the aerobic degradation of phenanthrene. Chemosphere, 286, 131709. https://doi.org/10.1016/J.CHEMOSPHERE.2021.131709

9. Figures

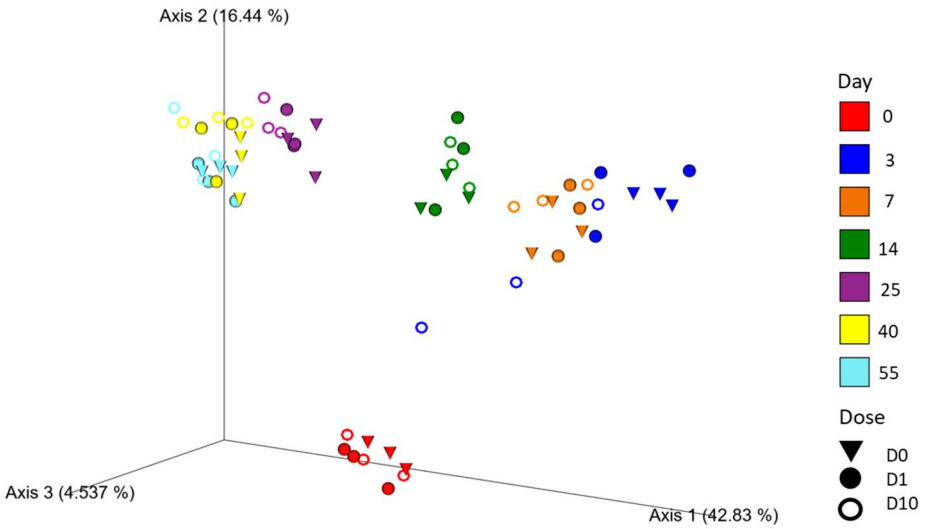

Figure 1: Principal coordinates analysis (PCoA) of the weighted Unifrac distance matrix of 16S rRNA *v3-v4 region* amplicon sequence variants (ASVs) showing the evolution of the bacterial community composition in control (D0) and tembotrione-treated soil microcosms (D1 and D10) after 0; 7; 14; 25; 40; and 55 days of incubation. The percentage of variance explained by each axis is given.

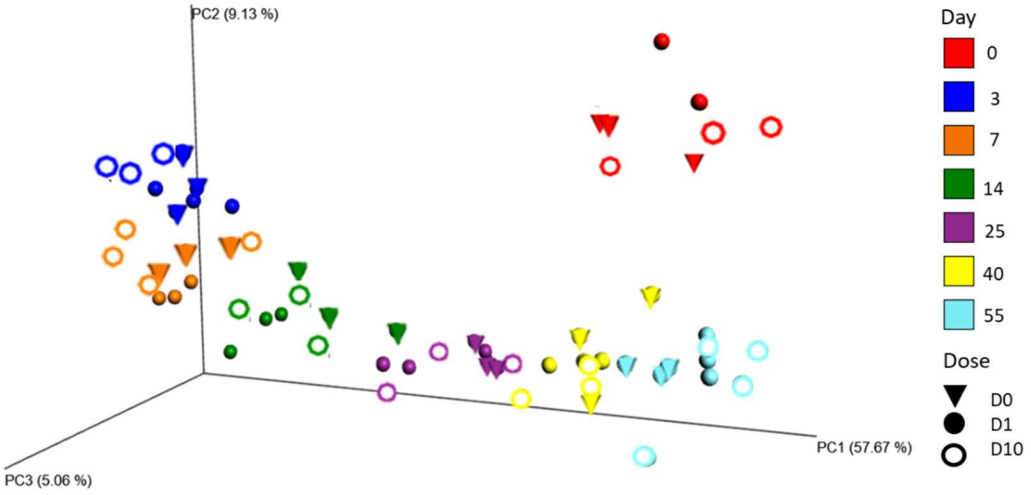

819 Figure 2: Principal coordinates analysis (PCoA) of the weighted Unifrac distance matrix of
820 HPPD sequences showing the evolution of the *hppd* community composition in control (D0)
821 and tembotrione-treated soil microcosms (D1 and D10) after 0; 7; 14; 25; 40 and 55 days of
822 incubation. The percentage of variance explained by each axis is given.

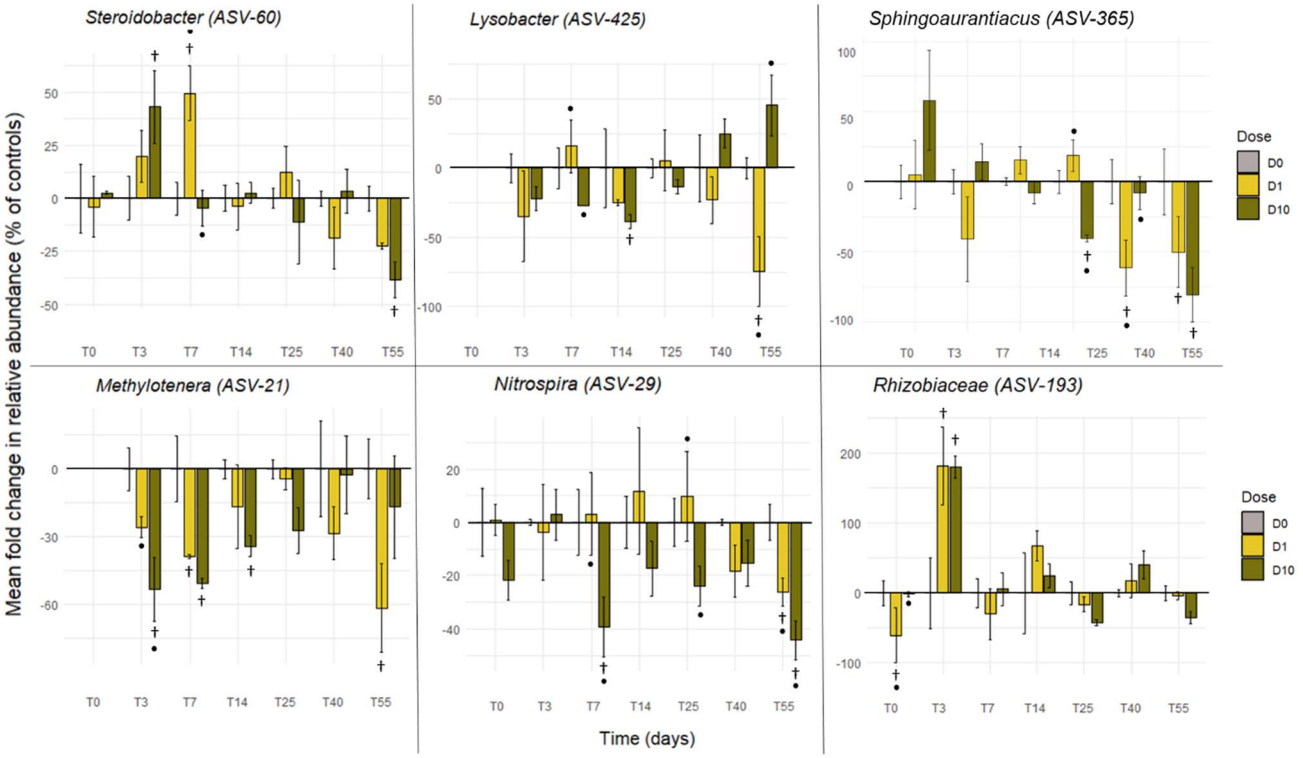

823

Figure 3: Mean fold changes in relative abundance for 16S rRNA ASVs identified by a GLMM analysis and discriminant between treatments (control: D0, tembotrione: D1 or D10) and sampling time (T0; T3; T7; T14; T25; T40; and T55). Taxonomic affiliations and ASV number in the dataset are indicated at the top of each plot. Fold changes are expressed as % relative abundance of control for each sampling time. Error bars are standard errors of mean values (n=3) and are shown also for controls with mean = 0%. Significant differences between

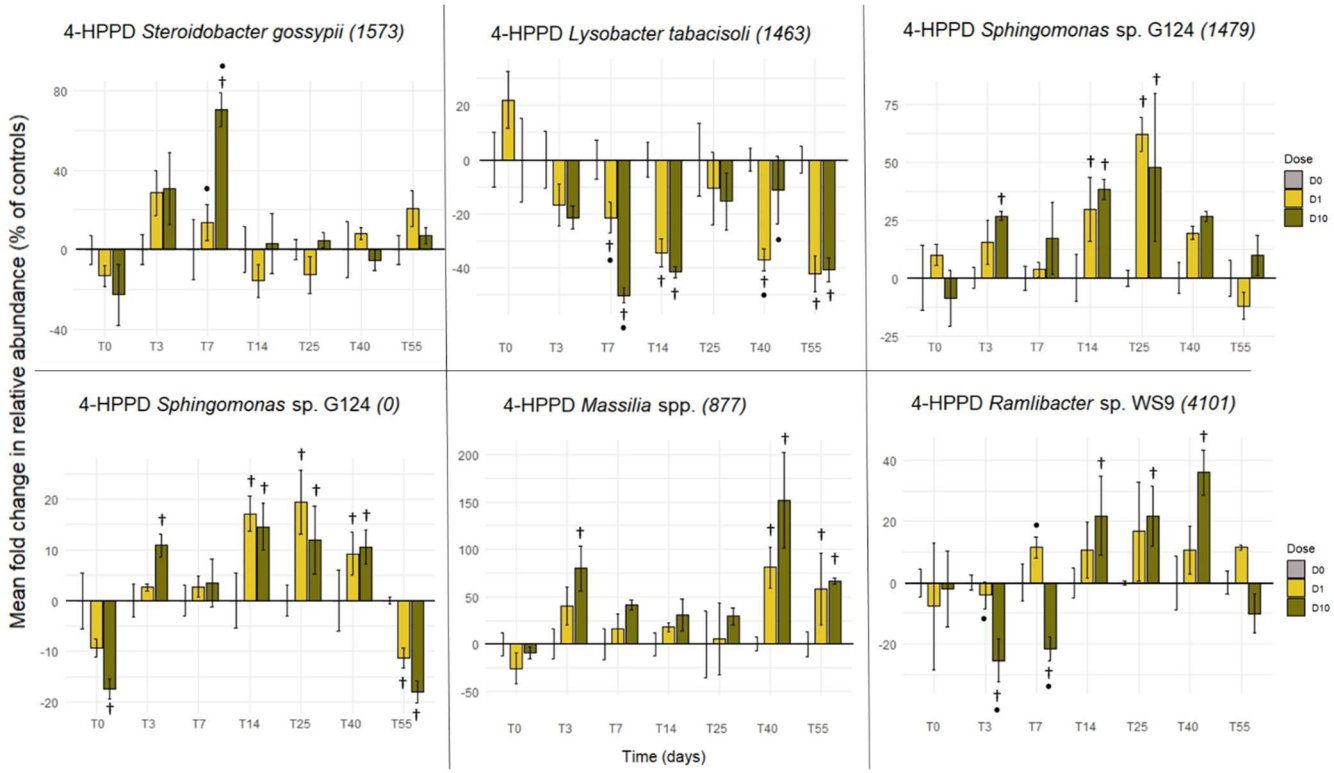

treatments and controls are indicated by the (†) symbol. Significant differences between treatments are indicated by the (•) symbol (pairwise test, $p \leq 0{,}05$)

Figure 4: Mean fold changes in relative abundance for HPPD cluster sequences identified by a GLMM analysis and discriminant between treatments (control: D0, tembotrione: D1 or D10) and sampling time (T0; T3; T7; T14; T25; T40; and T55). BLASTP results of amino-acid sequences for each HPPD cluster and its number in the dataset are indicated at the top of each plot. Fold changes are expressed as % relative abundance of control for each sampling time. Error bars are standard errors of mean values (n=3) and are shown also for controls with

839 mean = 0%. Significant differences between treatments and controls are indicated by the (†)
840 symbol. Significant differences between treatments are indicated by the (•) symbol (pairwise
841 test, $p \leq 0,05$)

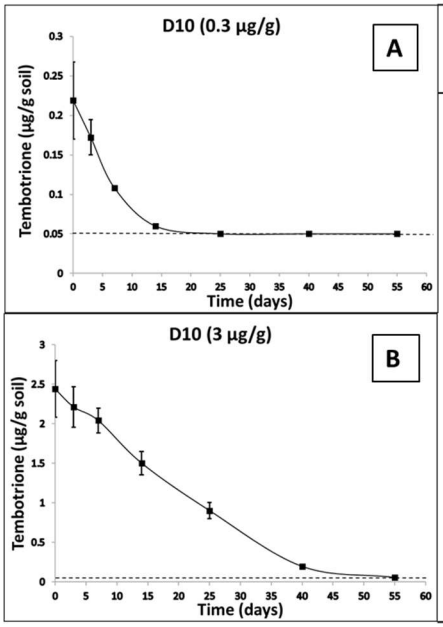

Single First Order (SFO) Kinetics of tembotrione dissipation — C

RfD	1	10
C_0 (µg/g)[a]	0.22	2.56
k (day^{-1})[b]	0.096	0.045
DT_{50} (days)[c]	7.2	15.3
DT_{90} (days)[c]	23.9	50.9
Error level X^2 (%)	2.6	8.4

842

843 Figure 5: Dissipation curves of tembotrione in soil microcosms treated with: D1 (A) and D10
844 (B). Mean concentrations (µg/g soil) of tembotrione are given for each day. Errors bars are the
845 standard errors (n=3). The limit of detection (L.O.D.) is indicated by a dotted line. Single First
846 Order (SFO) kinetics of tembotrione dissipation in soil microcosms (a: C_0 = initial
847 concentration; b : k = kinetic rate constant ; c : DT = Dissipation Time for 50% or 90%
848 dissipation) (C).

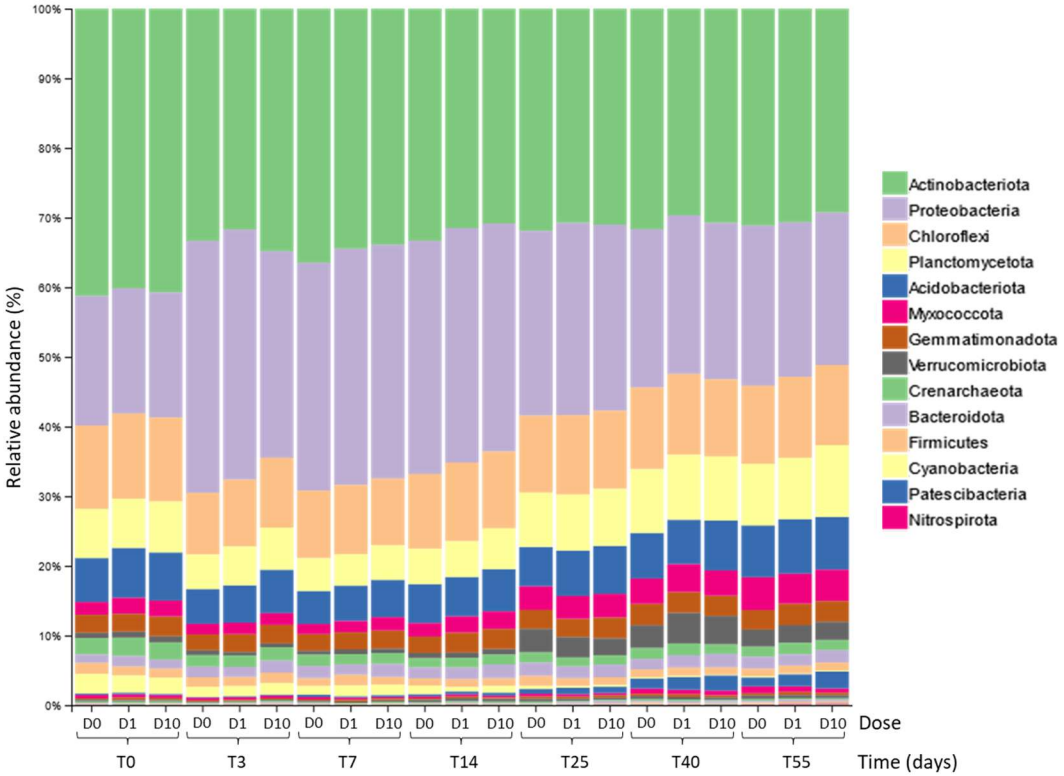

Figure S1: Relative abundance of microbial phyla (expressed as % of the total frequency of 16S rRNA ASVs) in soil microcosms for each sampling time (T0; T3; T7; T14; T25; T40 and T55) and treatments (control: D0, tembotrione: D1, D10).

Table S1: Alpha-diversity indices of soil bacterial community calculated for each sampling date (0; 3; 7; 14; 40; and 55 days) after treatment (control: D0, tembotrione: D1 or D10). Mean values ± standard error are shown. Different letters indicate significant differences between treatment at each time point (post-hoc Tukey's test, $p \leq 0,05$).

Time (days)	Treatment	Chao1	Phylogenetic diversity	Dominance ($*10^{-4}$)
0	D0	954 ± 116	74 ± 2	32 ± 3.7
	D1	961 ± 81	72 ± 6	30 ± 1.5
	D10	1127 ± 43	73 ± 2	28 ± 1.5
3	D0	960 ± 61	73 ± 1	148 ± 14.2 **a**
	D1	1029 ± 116	78 ± 6	132 ± 22.1 **a**
	D10	1094 ± 86	75 ± 1	40 ± 15 **b**
7	D0	825 ± 109	78 ± 10	74 ± 8
	D1	923 ± 26	76 ± 1	78 ± 2.5
	D10	1126 ± 24	85 ± 7	72 ± 5.1
14	D0	773 ± 82	71 ± 4	53 ± 0.7
	D1	904 ± 55	75 ± 6	55 ± 2.5
	D10	1092 ± 86	82 ± 5	53 ± 3.5
25	D0	1090 ± 14 **a**	79 ± 3	28 ± 0.4
	D1	1067 ± 157 **a**	77 ± 6	33 ± 3.9
	D10	1555 ± 81 **b**	106 ± 2	23 ± 0.6
40	D0	1348 ± 115	114 ± 7	22 ± 1.3
	D1	1311 ± 90	92 ± 6	23 ± 1.3
	D10	1423 ± 32	106 ± 7	21 ± 1
55	D0	1051 ± 71	82 ± 8 **a**	27 ± 0.7
	D1	1219 ± 31	106 ± 8 **ab**	25 ± 0.5
	D10	1430 ± 129	125 ± 10 **b**	21 ± 1.4

Table S2: Alpha-diversity indices of soil HPPDs calculated for each sampling date (0; 3; 7; 14; 40; and 55 days) after treatment (control: D0, tembotrione: D1 or D10). Mean values ± standard error are shown. Different letters indicate significant differences between treatment at each time point (post-hoc Tukey's test, $p \leq 0,05$).

Time (days)	Treatment	Observed HPPD	Phylogenetic Diversity	Simpson reciprocal
0	D0	532 ± 6 **ab**	133 ± 1 **ab**	48.7 ± 0.3 **ab**
	D1	559 ± 2 **a**	139 ± 1 **a**	56.4 ± 1.1 **a**
	D10	521 ± 2 **b**	131 ± 1 **b**	54.4 ± 1.2 **b**
3	D0	501 ± 5	124 ± 1	35.7 ± 1.6
	D1	491 ± 5	124 ± 1	35.9 ± 0.7
	D10	490 ± 8	123 ± 1	33.2 ± 1
7	D0	501 ± 8	125 ± 2	35.4 ± 1.6
	D1	486 ± 2	122 ± 1	35 ± 1.1
	D10	476 ± 7	118 ± 2	33.1 ± 3.2
14	D0	521 ± 3	131 ± 1 **a**	42.3 ± 1.4
	D1	506 ± 7	125 ± 1 **ab**	37.5 ± 2.3
	D10	498 ± 1	124 ± 1 **b**	38 ± 0.4
25	D0	535 ± 5	133 ± 2	52.2 ± 0.6 **a**
	D1	531 ± 5	133 ± 1	43 ± 1.9 **b**
	D10	520 ± 9	131 ± 2	49.4 ± 2.3 **ab**
40	D0	552 ± 7	138 ± 1	49.5 ± 1.1
	D1	528 ± 4	133 ± 1	45.6 ± 1.5
	D10	512 ± 1	131 ± 1	45 ± 0.9
55	D0	538 ± 9 **a**	139 ± 2	50.1 ± 0.1
	D1	540 ± 5 **ab**	139 ± 0.5	54.4 ± 1.1
	D10	556 ± 11 **b**	140 ± 1	54.4 ± 0.5

Table S3 (next page): List and taxonomic affiliations of 16S rRNA ASVs identified by the GLMM model with differential abundance analysis. Taxonomic affiliations of 16S rRNA ASVs were done using the SILVA 138 database and « feature classifier » tool of QIIME2. Confidence of identification is shown (max = 1).

Discriminant 16S rRNA ASVs identified by GLMM analysis	Taxonomic identification, baed on SILVA 138 database for 16S rRNA (domain; phylum; class; order; family; genus; species)	Confidence of identification
ASV-3	Bacteria; Proteobacteria; Gammaproteobacteria; Burkholderiales; Methylophilaceae; Methylotenera	0.9991
ASV-5	Bacteria; Proteobacteria; Alphaproteobacteria; Azospirillales; Azospirillaceae; Skermanella	0.9999
ASV-15	Bacteria; Actinobacteriota; Rubrobacteria; Rubrobacterales; Rubrobacteriaceae; Rubrobacter; uncultured bacterium	0.7002
ASV-21	Bacteria; Proteobacteria; Gammaproteobacteria; Burkholderiales; Methylophilaceae; Methylotenera	0.9948
ASV-29	Bacteria; Nitrospirota; Nitrospiria; Nitrospirales; Nitrospiraceae; Nitrospira; uncultured soil	0.8774
ASV-33	Bacteria; Chloroflexi; Gitt-GS-136; Gitt-GS-136; Gitt-GS-136; Gitt-GS-136	1.0000
ASV-38	Bacteria; Proteobacteria; Alphaproteobacteria; Sphingomonadales; Sphingomonadaceae	1.0000
ASV-52	Bacteria; Actinobacteriota; Acidimicrobiia; Microtrichales; Ilumatobacteraceae; uncultured	0.9684
ASV-104	Bacteria; Chloroflexi; Chloroflexia; Thermomicrobiales; JG30-KF-CM45; JG30-KF-CM45; uncultured bacterium	0.9716
ASV-138	Bacteria; Actinobacteriota; Acidimicrobiia; Microtrichales; Iamiaceae; Iamia	0.9996
ASV-222	Bacteria; Proteobacteria; Alphaproteobacteria; Acetobacterales; Acetobacteraceae; Craurococcus-Caldovatus; uncultured bacterium	0.7224
ASV-234	Bacteria; Planctomycetota; Phycisphaerae; Tepidisphaerales; WD2101 soil group; WD2101 soil group; uncultured bacterium	0.7130
ASV-365	Bacteria; Proteobacteria; Alphaproteobacteria; Sphingomonadales; Sphingomonadaceae; Sphingoaurantiacus	0.9999
ASV-425	Bacteria; Proteobacteria; Gammaproteobacteria; Xanthomonadales; Xanthomonadaceae; Lysobacter	1.0000
ASV-500	Bacteria; Bacteroidota; Bacteroidia; Cytophagales; Microscillaceae; uncultured	0.7744
ASV-568	Bacteria; Proteobacteria; Gammaproteobacteria; Burkholderiales; Methylophilaceae; MM2; uncultured bacterium	0.9986
ASV-784	Bacteria; Actinobacteriota; Actinobacteria; Propionibacteriales; Nocardioidaceae; Nocardioides	1.0000
ASV-20	Bacteria; Actinobacteriota; Actinobacteria; Micrococcales; Microbacteriaceae; Agromyces; Agromyces ramosus	0.8600
ASV-54	Bacteria; Myxococcota; bacteriap25; bacteriap25; bacteriap25; bacteriap25	0.7118
ASV-60	Bacteria; Proteobacteria; Gammaproteobacteria; Steroidobacterales; Steroidobacteraceae; Steroidobacter	0.9514
ASV-193	Bacteria; Proteobacteria; Alphaproteobacteria; Rhizobiales; Rhizobiaceae	1.0000
ASV-194	Bacteria; Planctomycetota; Phycisphaerae; Tepidisphaerales; WD2101 soil group; WD2101 soil group; uncultured bacterium	0.7968
ASV-219	Bacteria; Actinobacteriota; Acidimicrobiia; IMCC26256; IMCC26256; IMCC26256; uncultured Acidimicrobiia	0.7517
ASV-226	Bacteria; Gemmatimonadota; Gemmatimonadetes; Gemmatimonadales; Gemmatimonadaceae; Gemmatimonas	1.0000
ASV-270	Bacteria; Actinobacteriota; Actinobacteria; 0319-7L14; 0319-7L14; 0319-7L14; uncultured actinobacterium	0.9901
ASV-316	Bacteria; Actinobacteriota; Thermoleophilia; Gaiellales; Gaiellaceae; Gaiella; uncultured bacterium	0.8596

886 Table S4: List and taxonomic affiliations of discriminant HPPD clusters identified by GLMM
887 model with differential abundance analysis. *Blastp* was performed on amino acid sequences
888 of HPPD clusters, and the hits with best score are shown.

889

Discriminant HPPD clusters identified by GLMM analysis (n°)	BLASTP best hit	BLASTP score	BLASTP expect value	Accession number of best hit HPPD sequence
158	4-hydroxyphenylpyruvate dioxygenase [Microvirga sp. KLBC 81]	151 bits(382)	3.00E-42	WP_116528755.1
834	4-hydroxyphenylpyruvate dioxygenase [Massilia sp. PAMC28688]	161 bits(408)	3.00E-46	WP_219883008.1
877	MULTISPECIES: 4-hydroxyphenylpyruvate dioxygenase [unclassified Massilia]	156 bits(394)	4.00E-44	WP_182988546.1
1304	4-hydroxyphenylpyruvate dioxygenase [Massilia sp. Root351]	167 bits(423)	2.00E-48	WP_057158391.1
1351	4-hydroxyphenylpyruvate dioxygenase [Vitiosangium sp. GDMCC 1.1324]	140 bits(353)	3.00E-38	WP_108066616.1
1399	4-hydroxyphenylpyruvate dioxygenase [Pseudoduganella rivuli]	128 bits(321)	2.00E-33	WP_154380629.1
1463	4-hydroxyphenylpyruvate dioxygenase [Lysobacter tabacisoli]	162 bits(409)	2.00E-46	WP_196778621.1
1479	4-hydroxyphenylpyruvate dioxygenase [Sphingomonas sp. G124]	149 bits(375)	2.00E-41	WP_235067680.1
1568	4-hydroxyphenylpyruvate dioxygenase [Proteobacteria bacterium]	145 bits(367)	2.00E-40	MBS0379841.1
1646	4-hydroxyphenylpyruvate dioxygenase [Steroidobacteraceae bacterium]	134 bits(338)	6.00E-36	MBC8027036.1
0	4-hydroxyphenylpyruvate dioxygenase [Sphingomonas sp. G124]	162 bits(410)	1.00E-46	WP_235067680.1
123	4-hydroxyphenylpyruvate dioxygenase [Massilia sp. TS11]	142 bits(359)	7.00E-39	WP_237807894.1
211	4-hydroxyphenylpyruvate dioxygenase [Methylobacterium indicum]	124 bits(311)	8.00E-32	WP_058617985.1
669	4-hydroxyphenylpyruvate dioxygenase [Massilia sp. 9I]	161 bits(407)	4.00E-46	WP_201303265.1
728	4-hydroxyphenylpyruvate dioxygenase [Massilia sp. LPB0304]	155 bits(393)	5.00E-44	WP_193685763.1
1310	4-hydroxyphenylpyruvate dioxygenase [Massilia sp. PAMC28688]	162 bits(409)	3.00E-46	WP_219883008.1
1464	4-hydroxyphenylpyruvate dioxygenase [Sphingomonas segetis]	154 bits(390)	1.00E-43	WP_155263959.1
1470	4-hydroxyphenylpyruvate dioxygenase [Sphingomonas sp.]	156 bits(395)	2.00E-44	MBA2466995.1
1553	4-hydroxyphenylpyruvate dioxygenase [Steroidobacter gossypii]	149 bits(376)	1.00E-41	WP_203165151.1
1564	4-hydroxyphenylpyruvate dioxygenase [Sphingomonas sp. G124]	156 bits(394)	3.00E-44	WP_235067680.1
1573	4-hydroxyphenylpyruvate dioxygenase [Steroidobacter gossypii]	144 bits(364)	8.00E-40	WP_203165151.1
2819	4-hydroxyphenylpyruvate dioxygenase [Actinomycetia bacterium]	134 bits(338)	5.00E-36	MBV9254971.1
2821	4-hydroxyphenylpyruvate dioxygenase [Streptomyces sporangiiformans]	164 bits(414)	4.00E-47	WP_119102138.1
4101	4-hydroxyphenylpyruvate dioxygenase [Ramlibacter sp. WS9]	154 bits(389)	2.00E-43	WP_141512490.1
4124	4-hydroxyphenylpyruvate dioxygenase [Ramlibacter lithotrophicus]	138 bits(348)	3.00E-37	WP_168109283.1
4134	4-hydroxyphenylpyruvate dioxygenase [Variovorax sp. SG517]	140 bits(354)	3.00E-38	WP_176668964.1
4121	4-hydroxyphenylpyruvate dioxygenase [Vogesella oryzae]	116 bits(291)	5.00E-29	WP_174875948.1

890

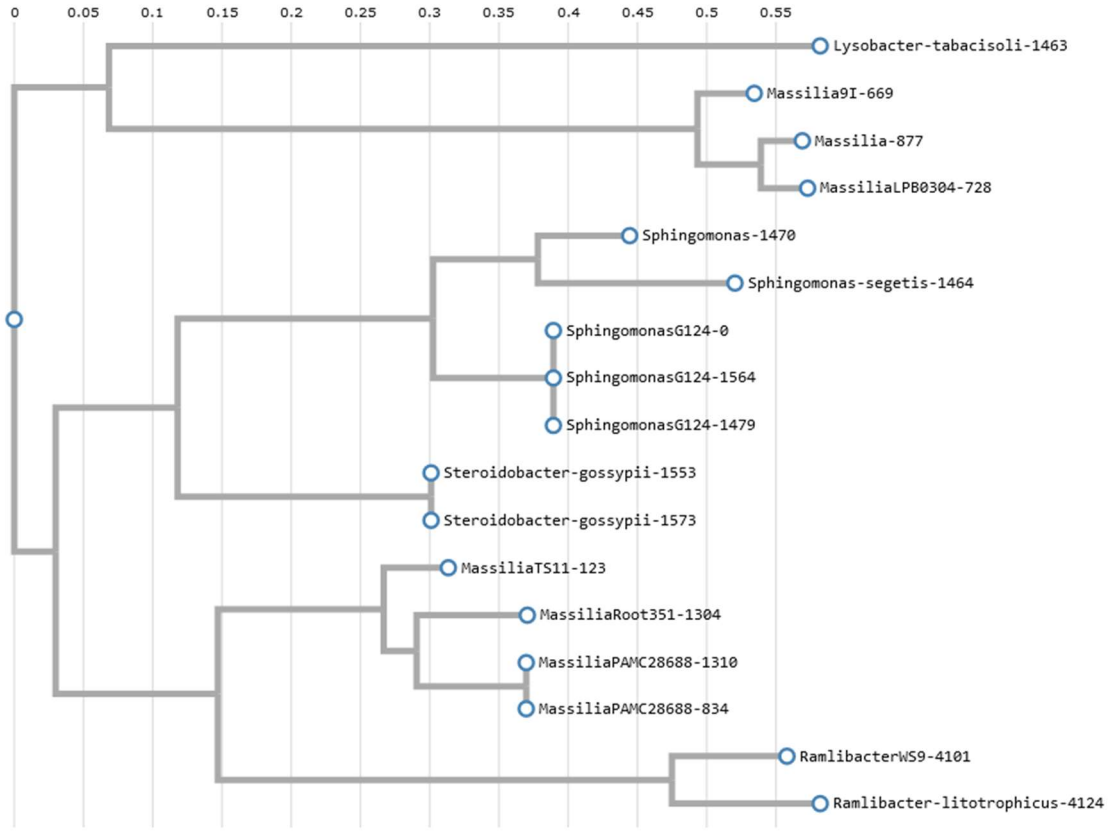

Figure S2: Phylogenetic tree of discriminant 4-HPPD sequences between tembotrione treatments in soil, identified by differential abundance analysis and a GLM Model. HPPD clusters from sequencing data and full protein sequences from the *Blastp* best hits were used for multiple sequence alignment and construction of the tree. Phylogenetic tree of the aligned sequences was constructed using FastTree v2.1.8 with default parameters.